PHYSICAL REVIEW C **76**, 041303(R) (2007)

New information on excited states below the μs isomer in ^{136}Sb

G. S. Simpson,* J. C. Angelique, J. Genevey, and J. A. Pinston
LPSC, Université Joseph Fourier Grenoble 1, CNRS/IN2P3, Institut National Polytechnique de Grenoble, F-38026 Grenoble Cedex, France

A. Covello and A. Gargano
Dipartimento di Scienze Fisiche, Università degli Studi di Napoli Federico II and INFN, Complesso Universitario di Monte Sant'Angelo, Via Cintia, I-80126 Napoli, Italy

U. Köster
Institut Laue-Langevin, B. P. 156, F-38042 Grenoble Cedex 9, France

R. Orlandi
INFN, Laboratori Nazionali di Legnaro, Legnaro, Italy

A. Scherillo
Rutherford Appleton Laboratory, Chilton, Didcot OX11 0QX, United Kingdom
(Received 26 June 2007; published 26 October 2007)

New experimental information has been obtained on the μs isomeric cascade in the very neutron-rich ^{136}Sb using γ-ray and conversion-electron spectroscopy at the Lohengrin mass spectrometer of the Institut Laue-Langevin. Two new transitions have been observed and their multipolarities determined, resolving the question of the origin of the isomerism. The new level scheme is in good agreement with predictions of a realistic shell-model calculation. The isomeric state is tentatively assigned a spin and parity of 6^- and a proposed $\pi g_{7/2}\nu(f_{7/2})^3$ dominant configuration.

DOI: 10.1103/PhysRevC.76.041303 PACS number(s): 21.10.Tg, 23.20.Lv, 25.85.Ec, 27.60.+j

Introduction. The study of very neutron-rich nuclei around doubly magic ^{132}Sn is a subject of great interest, as it offers an opportunity for testing the basic ingredients of shell-model calculations, in particular the nucleon-nucleon effective interaction, when moving toward the neutron drip line. In this context, a considerable effort is currently being made to gain information on exotic nuclei beyond the $N = 82$ shell closure, with special attention focused on the Sb isotopes, which are most appropriate for testing the matrix elements of the proton-neutron interaction between valence nucleons in different major shells. Recently, new experimental information has been gained on the two isotopes ^{134}Sb [1,2] and ^{135}Sb [3,4]. This has stimulated shell-model studies [5,6] employing a two-body effective interaction derived from the CD-Bonn nucleon-nucleon (NN) potential [7], with no use of any adjustable parameter. The results of these realistic shell-model calculations are in very good agreement with the observed spectroscopic properties of both nuclei. These results, considered along with those obtained for ^{134}Sn [8], have shown that there is no need to invoke shell-structure modifications to explain the presently available data on neutron-rich nuclei beyond ^{132}Sn.

On the above grounds, it is of key importance to try to take further steps in approaching the neutron drip line. The nucleus ^{136}Sb, with an N/Z ratio of 1.67, is at present the most exotic open-shell nucleus beyond ^{132}Sn for which a spectroscopic study has been performed [9], leading to the observation of a μs isomeric state. In this study it was concluded that the isomer most likely is the $I^\pi = 6^-$ state originating from the $\pi g_{7/2}\nu(f_{7/2})^3$ configuration.

As mentioned above, the $\pi g_{7/2}\nu f_{7/2}$ multiplet observed in ^{134}Sb is very well reproduced by the shell-model calculations of Ref. [6]. The observation in ^{136}Sb of low-energy states arising from the $\pi g_{7/2}\nu(f_{7/2})^3$ configuration makes it possible to study the evolution of this multiplet when adding a pair of neutrons and allows further exploration of possible changes in nuclear structure properties.

In the work of Ref. [9] only one γ-ray transition of 173 keV was observed in coincidence with ^{136}Sb, which alone was not enough to explain the origin of μs isomerism. In Ref. [9] an unseen low-energy $E2$ transition was postulated to be responsible for the μs lifetime. In the present work this nucleus has been studied with an experimental setup capable of detecting low-energy conversion electrons and γ rays.

A description of the experimental method and the results are presented. Next there is an interpretation of these results in terms of our shell-model description.

Experimental method and results. Delayed γ rays and conversion electrons from ^{136}Sb were observed using the Lohengrin mass spectrometer at the high-flux reactor of the Institut Laue-Langevin, Grenoble. Mass 136 nuclei were produced by thermal-neutron-induced fission of a thin $7 \times 0.5\,\text{cm}^2$, 1 mg ^{241}Pu target. The Lohengrin mass spectrometer was used to select nuclei recoiling from the target, according

*simpson@lpsc.in2p3.fr

to their mass-to-ionic charge ratios (A/q). The flight time of the $A = 136$ nuclei through the spectrometer was around 2.3 μs. The energy of the fission fragments was detected in an ionization chamber, filled with isobutane gas at a pressure of 35 mb, allowing the identification of A/q. The chamber consisted of two regions of gas, $\Delta E1 = 9$ cm and $\Delta E2 = 6$ cm, separated by a Frisch grid. A 6 μm thick Mylar foil was placed at the end of the chamber. The pressure of the gas in the chamber was adjusted so that the fission products stopped in the last few μm of the foil. A few mm behind the foil, two adjacent, rectangular, liquid-nitrogen-cooled Si(Li) detectors were placed to detect X rays and conversion electrons. Each detector had an active area of 2×3 cm^2, was 4.5 mm thick, and could detect electrons down to about 20 keV in energy with an efficiency of 14.7%. γ rays de-exciting isomeric states, and states below the isomer, were detected by two Clover Ge detectors [10]. These detectors were placed perpendicular to the ion beam in a compact geometry, made possible as the ionization chamber was only 6 cm thick. The total γ-ray detection efficiency was 14.6 and 3.5% for photons of 100 keV and 1 MeV, respectively. Any γ rays detected in the Ge or Si detectors up to 20 μs after the arrival of an ion were recorded by the the data acquisition system. Measurements of delayed γ rays and conversion electrons from ^{136}Sb were an experimental challenge as the ionization chamber was unable to resolve the different isobars in the $A = 136$ mass chain. Another μs isomer exists in this mass chain, the 2.95 μs 6^+ state of ^{136}Xe [11], which is strongly produced with a fission yield of $8.6(3.1) \times 10^{-3}$ per fission [12]. ^{136}Sb, being far from stability, has a much weaker fission yield, $3.5(1.3) \times 10^{-4}$ per fission [12]. The previously measured short lifetime of the isomer, 565(50) ns [9], meant also that much of the intensity of the isomeric state decayed during the 2.3 μs flight time through the spectrometer. Hence, delayed γ-ray and conversion-electron spectra obtained in coincidence with $A = 136$ ions were dominated by transitions from the ^{136}Xe isomer. To best enhance the number of delayed transitions from ^{136}Sb, relative to ^{136}Xe, a coincidence time window of 1.5 μs, after the arrival of an ion, was used for all ion-γ and ion-conversion-electron/X-ray coincidences in the data analysis. Additionally within this 1.5 μs window, the time between any Si-Ge coincidences was limited to be less than 500 ns. These coincidence conditions were used throughout the whole data analysis.

In addition to the previously reported delayed 173 keV γ ray from ^{136}Sb [9], two new delayed transitions of 53.4(3) keV and 51.4(5) keV were observed. The 53.4 keV γ ray was observed in coincidence with Sb K_α X rays and $A = 136$ ions, as shown in Fig. 1. By gating on the 173.0 keV γ-ray transition, observed in the Ge detectors, and $A = 136$ ions it was possible to observe coincident conversion electrons at 47.1 keV (corrected for the energy loss in the Mylar foil), as shown in Fig. 2. These electrons correspond to the $L+M$ groups of the two new transitions. If they originated from a K group, then the conversion coefficient would be sufficiently small to allow a corresponding γ ray to be observed in the Ge detectors, which was not the case. Adding the weighted mean L binding energy (the dominant group) of 4.3 keV for Sb, and correcting for the energy loss in the Mylar,

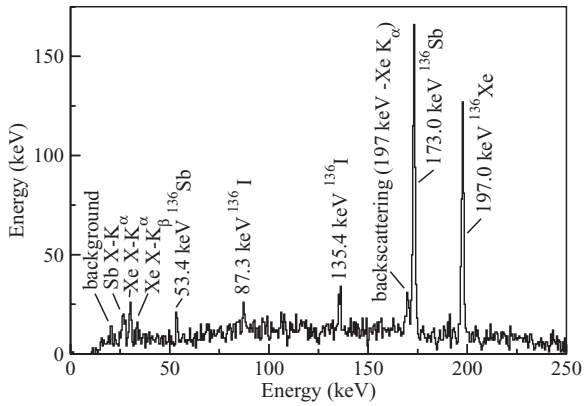

FIG. 1. γ rays observed in the Ge detectors in coincidence with K_α X rays measured in the Si detectors up to 1.5 μs after the arrival of an $A = 136$ ion. Background transitions are present from the strongly produced isomer in ^{136}Xe [11] and from ^{136}I, produced by β decay.

gives a transition energy of 51.4(5) keV. Because the two new transitions of 51.4 and 53.4 keV are close in energy, the electron line is composed of both transitions; however, one transition, the 51.4 keV one, is responsible for the majority of the intensity in this line. This is justified later. Further evidence that this peak consists of the $L+M$ groups is obtained by gating at the expected energy of the K electrons. The energy distribution of the K electrons, which were calculated to pass through ~2.5 μm of Mylar on average, was largely broadened, which when combined with the low statistics of this experiment and the rather high energy threshold meant no K electron peaks were observed. The thickness of Mylar traversed by the electrons was estimated by comparing the difference between detected known γ rays and conversion electrons and the tabulated values of the energy loss of electrons in Mylar [13]. The broadening was due to the large solid angle subtended

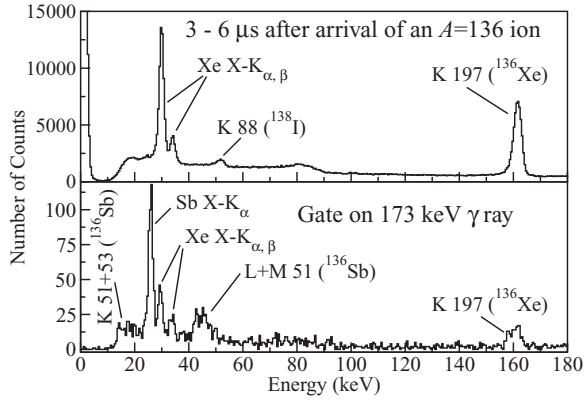

FIG. 2. Conversion electrons and X rays observed in the Si detectors, in the upper spectrum 3 to 6 μs after the arrival of an $A = 136$ ion and in the lower spectrum in coincidence with the 173.0 keV γ ray in the Ge detectors, 0 to 1.5 μs after the arrival of an $A = 136$ ion. A conversion-electron line of 47.1 keV is observed and is identified as the $L+M$ lines of a 51.4 keV transition from ^{136}Sb.

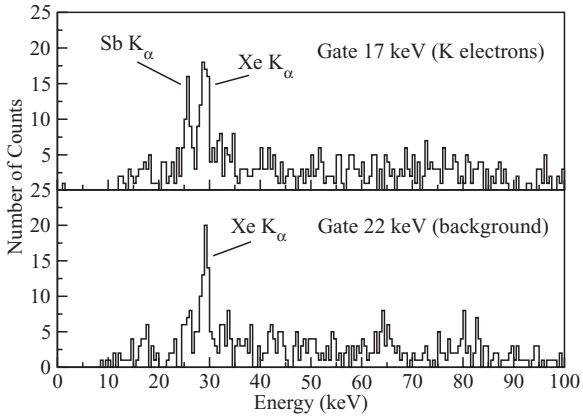

FIG. 3. Si-Si coincidence spectra obtained when gating on the expected energy (17 keV, including the energy loss of electrons in the Mylar foil) of K electrons from the 51.4 and 53.4 keV transitions. A gate on a good approximation to background (22 keV) is also shown, though some of the high energy tail of the K electron distribution is present.

by the Si detectors, which means that electrons detected in different regions of the detectors had passed through different thicknesses of Mylar. As the energy loss of electrons in Mylar changes rapidly below about 30 keV, electrons below this energy have strongly broadened peaks. An example of broadening at this electron energy with this technique is well illustrated in Fig. 2 of Ref. [14]. Gates set in a Si-Si coincidence matrix, shown in Fig. 3, at the expected energy of the K electrons (17 keV, when accounting for the 5 keV energy loss in the Mylar) show a clear coincidence with Sb X rays, unlike the background spectra.

Comparing the ratio of the intensity of 173.0 keV γ rays, detected in the Ge detectors, with the corresponding K electron intensity at 142 keV measured in the Si detectors, shown in Fig. 4, it was possible to measure an internal-conversion coefficient of $\alpha_K = 0.17(4)$ for this transition. This conversion coefficient is consistent with the theoretical value for an $E2$ multipolarity ($\alpha_K = 0.19$).

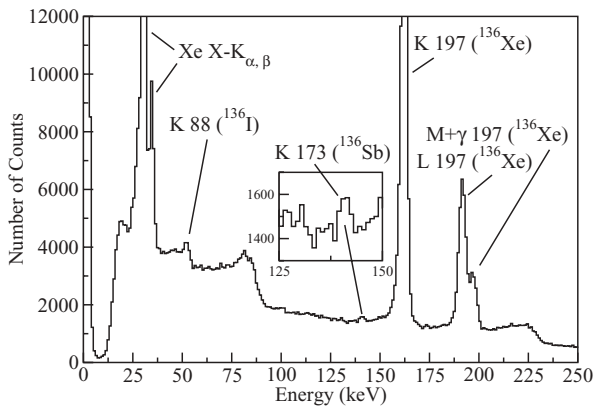

FIG. 4. Conversion electrons and X rays observed in the Si detectors 0 to 1.5 μs after the arrival of an $A = 136$ ion.

Examining the number of K_α X rays and the sum of the $L+M$ electrons in coincidence with the 173.0 keV γ ray, shown in Fig. 2, reveals a ratio of $I_{K_\alpha X}/I_{e(L+M)}$ of 1.7(4). This is inconsistent with the theoretical ratios of 0.78 for two $E2$ transitions, 5.6 for two $M1$ transitions, or 5.3 for two $E1$ transitions. Note, the previously mentioned ratios would be the same for only one transition. Hence, two low-energy transitions, in addition to the 173.0 keV $E2$, must be present in the isomeric-decay cascade. If two transitions, with different multipolarities, are considered, then the theoretical intensity ratios for $I_{K_\alpha X}/I_{e(L+M)}$, corrected for the X-ray-to-electron relative detection efficiency and fluorescence yield, are 5.5(3) for $M1$-$E1$, 1.4(1) for $E2$-$E1$, and 1.6(1) for $E2$-$M1$ transitions. Hence, the nature of these transitions is consistent with either $E2$-$E1$ or $E2$-$M1$.

By gating on Sb K_α X rays in the Si detectors, the ratio $I_\gamma(173.0)/I_\gamma(53.4)$ in the Ge detectors, shown in Fig. 1, was found to be 10.5(23). This measured ratio can then be compared to the theoretical ratios (corrected for the efficiency of the Ge detectors) of 7.2(5) for an $E2$-$E1$ cascade and 9.1(6) for an $E2$-$M1$ cascade showing the multipolarity of the 53.4 keV transition to be $M1$ in nature. Therefore, the 51.4 keV transition can be assigned to be $E2$ in nature. Returning to the experimentally measured 47.1 keV $L+M$ electron line, its intensity can now be calculated to consist of 82% from the 51.4 keV $E2$ and 18% from the 53.4 keV $M1$, using theoretical conversion coefficients, justifying *a posteriori* the use of the 51.4 keV $E2$ as the transition's dominant component.

The half-life of the isomeric state was obtained by summing time spectra from ion-γ coincidences between $A = 136$ ions and the 173.0 keV γ rays detected in the Clover Ge detectors and ion-X coincidences between $A = 136$ ions and the K_α X rays detected in the Si detectors. The half-life was measured to be 480(100) ns, as shown in Fig. 5, in agreement with 565(50) ns measured in Ref. [9].

Discussion. Motivated by the new spectroscopic information obtained from the present study, a shell-model calculation has been performed with the same realistic interaction used

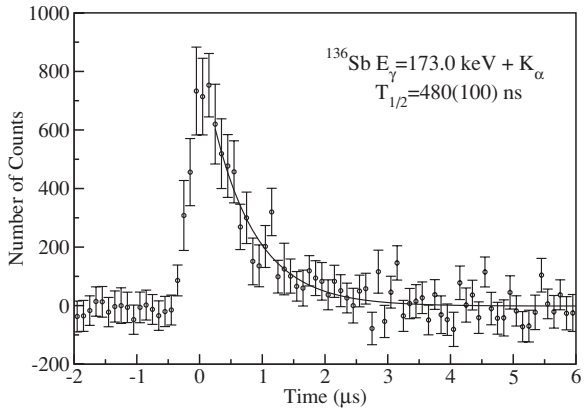

FIG. 5. Summed time spectra of gates on the 173.0 keV γ-ray transition detected in the Clover Ge detectors and the Sb K_α X rays in the Si detectors.

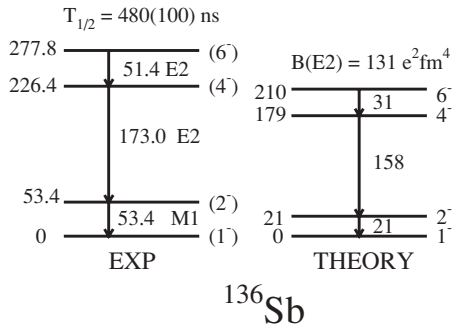

FIG. 6. Proposed decay scheme of the ^{136}Sb isomer.

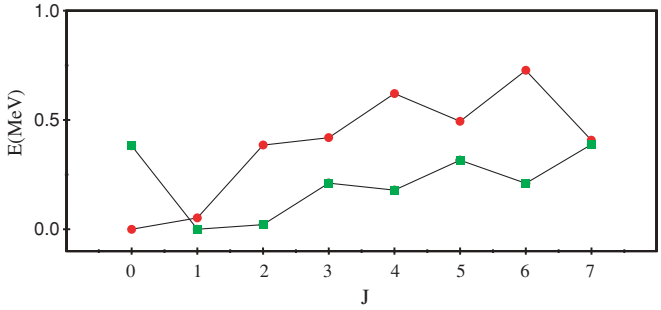

FIG. 7. (Color online) Low-lying calculated levels of ^{134}Sb (solid circles) and ^{136}Sb (solid squares). The lines are to guide the eye. See text for details.

for the lighter Sb isotopes and the theoretical predictions compared with the experimental data.

This shell-model study of ^{136}Sb was performed along the same lines as those used for ^{134}Sb and ^{135}Sb [5,6]. We assume that ^{132}Sn is a closed core and let the valence proton occupy the five levels $0g_{7/2}$, $1d_{5/2}$, $1d_{3/2}$, $0h_{11/2}$, and $2s_{1/2}$ of the 50–82 shell, while for the three valence neutrons the model space includes the six levels $1f_{7/2}$, $2p_{3/2}$, $0h_{9/2}$, $2p_{1/2}$, $1f_{5/2}$, and $0i_{13/2}$ of the 82–126 shell. The two-body effective interaction is derived from the CD-Bonn NN potential, the short-range repulsion of the latter being renormalized by use of the low-momentum potential $V_{\text{low-k}}$ [15]. Details of the derivation can be found in Ref. [8] and references therein. As regards the single-particle energies, they are taken from experimental values, as described in Ref. [5], where all the adopted values are reported. The shell-model calculation was performed using the OXBASH code [16].

The proposed experimental level scheme of ^{136}Sb is shown in Fig. 6, where it is compared with the calculated results. In this figure the first four calculated states are reported and we see that each of them has a counterpart in the experimental spectrum. The 51.4 keV $E2$ is almost certainly the $6^- \rightarrow 4^-$ isomeric transition, from lifetime arguments. The order of the 173 and 51.4 keV transitions was assigned by comparison with the calculation. The discrepancies between the experimental and the predicted excitation energies do not exceed 70 keV. Note that the ground state spin was already identified as 1^- in Ref. [17].

An important piece of information is provided by the measured half life of the 6^- state, from which a $B(E2; 6^- \rightarrow 4^-)$ value of 170(40) e^2 fm^4 = 4.2 W.u. is extracted. Using effective proton and neutron charges of 1.55 e and 0.70 e, respectively, we obtain the value 131 e^2 fm^4, which compares very well with experiment. It is worth mentioning that these values of the effective charges have been consistently used in our previous calculations for nuclei in the ^{132}Sn region [8].

To conclude this section, it is worth emphasizing that the new experimental information on ^{136}Sb puts our realistic effective Hamiltonian to a further test. The results presented here, along with those of our previous studies, show the ability of this Hamiltonian to consistently explain the available experimental data on neutron-rich nuclei beyond ^{132}Sn. This makes it challenging to present here predictions for ^{136}Sb, which, if new data become available, may be helpful to understand specific aspects of the effective nucleon-nucleon interaction.

The four observed levels in ^{136}Sb are all identified with states that are dominated by the configuration $\pi g_{7/2}\nu(f_{7/2})^3$. In Fig. 7 the yrast states with angular momentum from 0^- to 7^- are shown, which all arise from this configuration. These states may be viewed as the evolution of the $\pi g_{7/2}\nu(f_{7/2})$ multiplet in ^{134}Sb, which is shown in Fig. 7 for comparison.

One can see that the patterns for ^{134}Sb and ^{136}Sb are quite different, as was also noted in Ref. [9]. Both exhibit staggering, but with different magnitude and opposite phase. In ^{136}Sb, the ground state is predicted to have $J^\pi = 1^-$ while the 0^- is raised at about 380 keV, in contrast to the very small spacing between the 0^- ground state and the first excited 1^- state in ^{134}Sb (13 keV).

It is worth mentioning that the percentage of configurations other than the dominant one in the considered states of ^{136}Sb is rather large, ranging from 24 to 32%. The configuration mixing, however, does not affect significantly the behavior of the spectrum of ^{136}Sb shown in Fig. 7.

One may be surprised at the fact that an additional pair of neutrons can cause such rapid a change from the particle-particle spectrum of ^{134}Sb to a spectrum that is similar to the particle-hole one. Actually, the overall action of the neutron-proton interaction is significantly influenced by the presence of the two additional neutrons. We have verified that while the shift in the excitation energy of the 0^- state may be explained, as usual, by considering the two additional neutrons coupled to zero angular momentum, the role of components with a nonzero coupled pair is crucial in determining the calculated staggering. The presence of such components in the wave functions of the low-lying states is consistent with the low excitation energy of the 2^+ state as well as the 4^+ and 6^+ states in ^{134}Sn. This is a sign of a reduction in the neutron pairing interaction when crossing the $N = 82$ shell [18].

The observation of the missing states of the "$\pi g_{7/2}\nu(f_{7/2})$ multiplet" in ^{136}Sb is certainly needed to verify the soundness of the above findings. However, the level scheme resulting from the present experiment shows that there is no state with $J^\pi = 3^-, 5^-$, or 7^- below the isomeric 6^- state, which seems to confirm the theoretical predictions.

Summary. Delayed γ rays and conversion electrons have been measured in the very neutron-rich nucleus ^{136}Sb, which

represents a further step in the far-from-stability region beyond $N = 82$. The multipolarities of these transitions have been determined and a level scheme has been constructed by comparison with the results of a realistic shell-model calculation. The predicted energies and $B(E2; 6^- \rightarrow 4^-)$ are in very good agreement with measured values. This shows that a consistent shell-model description can be given of the presently known nuclei in this region.

The work at the University of Naples Federico II was supported in part by the Italian Ministero dell'Istuzione, dell'Università e della Ricerca (MUIR).

[1] J. Shergur, A. Wöhr, W. B. Walters, K. L. Kratz, O. Arndt, B. A. Brown, J. Cederkall, I. Dillmann, L. M. Fraile, P. Hoff *et al*., Phys. Rev. C **71**, 064321 (2005).

[2] A. Korgul, H. Mach, B. Fogelberg, W. Urban, W. Kurcewicz, T. Rzaca-Urban, P. Hoff, H. Gausemel, J. Galy, J. L. Durell *et al*., Eur. Phys. J. A **15**, 181 (2002).

[3] J. Shergur, A. Wöhr, W. B. Walters, K. L. Kratz, O. Arndt, B. A. Brown, J. Cederkall, I. Dillmann, L. M. Fraile, P. Hoff *et al*., Phys. Rev. C **72**, 024305 (2005).

[4] A. Korgul, H. Mach, B. A. Brown, A. Covello, A. Gargano, B. Fogelberg, R. Schuber, W. Kurcewicz, E. Werner-Malento, R. Orlandi *et al*., Eur. Phys. J. A **25**, S01, 123 (2005).

[5] L. Coraggio, A. Covello, A. Gargano, and N. Itaco, Phys. Rev. C **72**, 057302 (2005).

[6] L. Coraggio, A. Covello, A. Gargano, and N. Itaco, Phys. Rev. C **73**, 031302(R) (2006).

[7] R. Machleidt, Phys. Rev. C **63**, 024001 (2001).

[8] A. Covello, L. Coraggio, A. Gargano, and N. Itaco, Prog. Part. Nucl. Phys. **59**, 401 (2007).

[9] M. N. Mineva, M. Hellström, M. Bernas, J. Gerl, H. Grawe, M. Pfützner, P. H. Regan, M. Rejmund, D. Rudolph, F. Becker *et al*., Eur. Phys. J. A **11**, 9 (2001).

[10] G. Duchêne, F. A. Beck, P. J. Twin, G. de France, D. Curien, L. Han, C. W. Beausang, M. A. Bentley, P. J. Nolan, and J. Simpson, Nucl. Instrum. Methods A **432**, 90 (1999).

[11] A. A. Sonzogni, Nucl. Data Sheets **95**, 837 (2002).

[12] JEFF 3.1, Joint Evaluated Fission and Fusion Project, an evaluated database of fission and fusion data maintained by the NEA. http://www.nea.fr/html/dbdata.

[13] L. Pages, E. Bertel, H. Joffre, and L. Sklavenitis, Atomic Data **4**, 1 (1972).

[14] J. Genevey, J. A. Pinston, C. Foin, M. Rejmund, H. Faust, and B. Weiss, Phys. Rev. C **65**, 034322 (2002).

[15] S. Bogner, T. T. S. Kuo, L. Coraggio, A. Covello, and N. Itaco, Phys. Rev. C **65**, 051301(R) (2002).

[16] B. A. Brown, A. Etchegoyen, and W. D. M. Rae, The computer code OXBASH, MSU-NSCL, Report No. 524, 1988.

[17] P. Hoff, J. P. Omtvedt, B. Fogelberg, H. Mach, and M. Hellström, Phys. Rev. C **56**, 2865 (1997).

[18] J. Terasaki, J. Engel, W. Nazarewicz, and M. Stoitsov, Phys. Rev. C **66**, 054313 (2002).